Networks of Triboelectric Nanogenerators for Harvesting Water Wave Energy: A Potential Approach toward Blue Energy

Jun Chen,[†,⊥] Jin Yang,[†,‡,⊥] Zhaoling Li,[†,§,⊥] Xing Fan,[†] Yunlong Zi,[†] Qingshen Jing,[†] Hengyu Guo,[†] Zhen Wen,[†] Ken C. Pradel,[†] Simiao Niu,[†] and Zhong Lin Wang*[,†,∥]

[†]School of Materials Science and Engineering, Georgia Institute of Technology, Atlanta, Georgia 30332-0245, United States, [‡]Department of Optoelectronic Engineering, Chongqing University, Chongqing 400044, China, [§]Key Laboratory of Science & Technology of Eco-Textile, College of Textiles, Donghua University, Shanghai 201620, China, and [∥]Beijing Institute of Nanoenergy and Nanosystems, Chinese Academy of Sciences, Beijing 100083, China. [⊥]These authors contributed equally to this work.

ABSTRACT With 70% of the earth's surface covered with water, wave energy is abundant and has the potential to be one of the most environmentally benign forms of electric energy. However, owing to lack of effective technology, water wave energy harvesting is almost unexplored as an energy source. Here, we report a network design made of triboelectric nanogenerators (TENGs) for large-scale harvesting of kinetic water energy. Relying on surface charging effect between the conventional polymers and very thin layer of metal as electrodes for each TENG, the TENG networks (TENG-NW) that naturally float on the water surface convert the slow, random, and high-force oscillatory wave energy into electricity. On the basis of the measured output of a single TENG, the TENG-NW is expected to give an average power output of 1.15 MW from 1 km^2 surface area. Given the compelling features, such as being lightweight, extremely cost-effective, environmentally friendly, easily implemented, and capable of floating on the water surface, the TENG-NW renders an innovative and effective approach toward large-scale blue energy harvesting from the ocean.

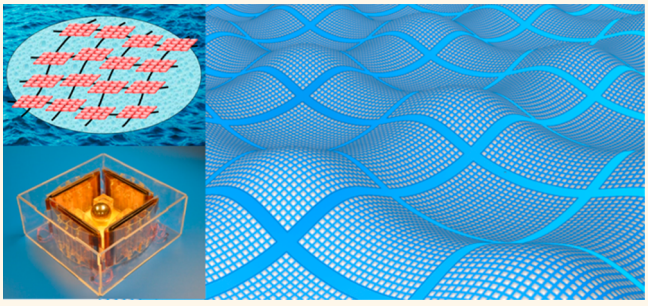

KEYWORDS: triboelectrification · TENG-NW · blue energy harvesting

Searching for renewable energy with reduced carbon emissions is mandatory for the sustainable development of human civilization. In the past decades, increased research efforts have been committed to seek for clean and renewable energy sources as well as to develop renewable energy technologies.[1] Water wave, wind, and solar irradiance, available in huge quantities, are clean and renewable energy sources with great potential.[2,3] In comparison with solar and wind energy, energy from water waves in the ocean may have several advantages.[4−6] Widely distributed across the globe, water kinetic energy is one of the richest energy sources for large-scope applications. The energy provided by water waves has a much less dependence on season, day or night, weather, and/or temperature. Although numerous studies have concluded that water wave power could contribute massive amounts to the overall energy consumption of the world, the utilization of water wave energy is way underexplored.[4−7]

The general approach for harvesting mechanical kinetic energy is mainly based on electromagnetic effect, which, however, is likely to have possible limitations for harvesting water wave energy in the ocean. First, the electromagnetic generator (EMG) is usually heavy and has a large mass density owing to the presence of magnets and metal coils, so it cannot naturally float on the surface of the water unless supported by a floater or a buoy platform. In ocean, the most dynamic energy presents at the surface of water. Second, the EMG is most

* Address correspondence to zhong.wang@mse.gatech.edu.

Received for review January 24, 2015 and accepted February 21, 2015.

Published online 10.1021/acsnano.5b00534

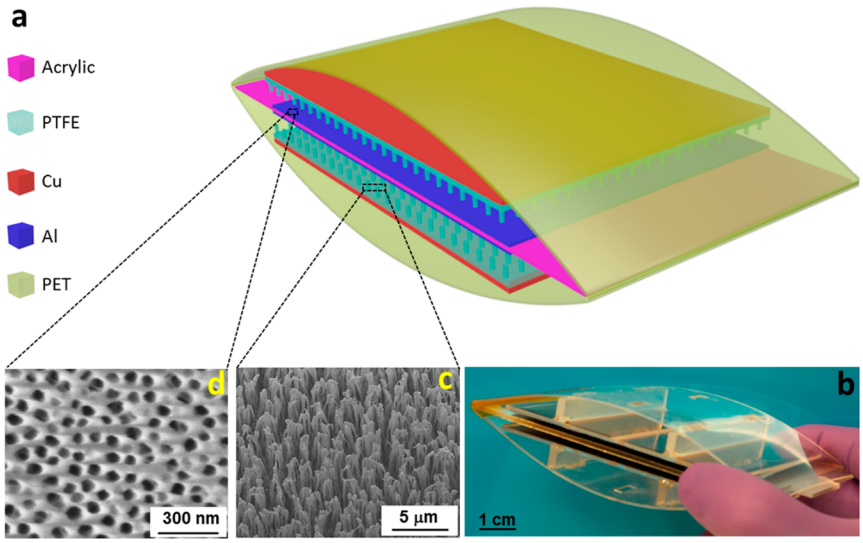

Figure 1. Single unit in a TENG. (a) Schematic illustration and (b) photograph of an as-fabricated minimum functional unit. (c) SEM image of PTFE nanowires. (d) SEM image of nanopores on aluminum electrode.

effective to catch the power from a flowing stream, so that the wave energy of water cannot be effectively harvested. Lastly, the fabrication of EMG requires high-quality materials, so that it may not be cost-effective for applications at a large surface area.[4−8]

Recently, a new type of generator has been invented based on the triboelectricity utilizing conventional organic materials, so that it is light, extremely low-cost, easy to fabricate, and easy to be scaled up.[9−22] The triboelectric nanogenerator (TENG) can give an instantaneous energy conversion efficiency as high as 55%.[23] In this work, we presented a TENG network (TENG-NW) design as a potential approach for harvesting large-scale water wave energy. Relying on the surface contact electrification effect between the conventional polymers and very thin layer of metal as electrodes, the TENG-NW is extremely lightweight, low-cost, high anticorrosion to the marine environment, and capable of floating on the surface of water for wave energy harvesting. By using the collision of a rolling ball caused contact and separation, the TENG converts the slow, random and high-force all-directional oscillatory motions into electricity. An average power output of 1.15 MW is expected to be generated from one kilometer square water surface in nature. Given the extremely low cost and unique applicability resulting from distinctive mechanism and simple structure, the TENG-NW renders a green alternative to traditional methods potentially for large-scale blue energy harvesting.

RESULTS AND DISCUSSION

The basic unit of the TENG has arch-shaped top and bottom plates with a multilayer core, as schematically shown in Figure 1a. Both the top and bottom plates are made of polyethylene terephthalate, naturally bent by a heat treatment, which helps to carry out the action of effective charge separation and contact using the elasticity of the film. A photograph of an as-fabricated unit is shown in Figure 1b. Holding a sandwiched structure, both the upper and bottom layers of the functional core is polytetrafluoroethylene (PTFE) film with deposited copper as back electrodes. PTFE nanowire arrays were created on the exposed PTFE surface by a top-down method through reactive ion etching, which largely enhances the charge density of contact electrification.[24,25] A scanning electron microscopy (SEM) image of vertically aligned PTFE nanowires is displayed in Figure 1c, which indicates that the average clustering diameter of FEP nanowires is 54 ± 3 nm with an average length of 1.5 ± 0.5 μm. Aluminum thin film with nanoporous surface is sandwiched between the top and bottom layers of the functional core, playing dual roles as an electrode and a contact surface. An SEM image of nanopores on the aluminum is presented in Figure 1d. The average diameter and depth of the aluminum nanopores are 57 ± 5 nm and 0.8 ± 0.2 μm, respectively, with a distribution density of 212 per μm^2. Acrylic was selected as the structural supporting material owing to its decent strength, lightweight, good machinability, and low cost.

The fundamental working principle of the reported TENG is based on the coupling between contact electrification and electrostatic induction,[26−30] as depicted in Figure 2. Here, both two-dimensional schematic illustrations of charge distribution (up) and potential distribution by COMSOL (down) were used for interpretation. When an external force, for example, the collision from a rolling ball, is applied to the top plate of the minimum functional unit, which brings the two layers of PTFE into contact with middle aluminum simultaneously, charge transfer occurs at the contact interfaces.[31−36] According to the triboelectric series, electrons are injected from aluminum into PTFE since

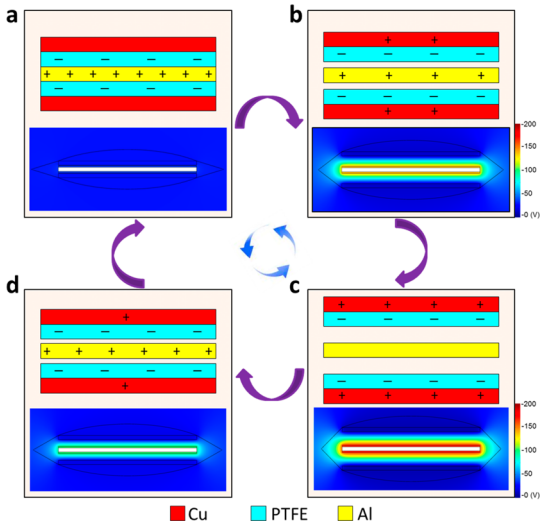

Figure 2. Schematics of operating principle of the TENG. Both two-dimensional schematic illustrations of the charge distribution (up) and potential distribution by COMSOL (down) were employed to elucidate the working principle of the minimum functional unit. (a) Initial state in which the PTFE is negatively charged after contact with aluminum. (b) When the PTFE and aluminum separates, electric potential difference drives the electrons from back electrodes to the contact electrode, screening the triboelectric charges and leaving behind the inductive charges. (c) With continuously increasing the separation, all the positive triboelectric charges were almost entirely screened. (d) Reduced separation between the contact surfaces will drive the free electrons to flow back to the copper electrode until the two contact surfaces come into contact. Note: Aluminum nanopores and PTFE nanowires are not shown in the sketch for the simplification of illustration.

PTFE is much more triboelectrically negative than aluminum, generating positive triboelectric charges on the aluminum and negative ones on the PTFE (Figure 2a). Subsequently, if the collision disappears, the elasticity of the arch-shaped plates will lead to a separation between the PTFE and the aluminum. As a result, the positive triboelectric charges and the negative ones no longer coincide on the same plane and generate an inner dipole moment between the two sets of contact surfaces. Such a dipole moment drives free electrons from the copper electrode to the aluminum electrode to balance out the electric field, producing positively induced charges on the copper electrode (Figure 2b). The flow of electrons lasts until the upper plate reaches the highest point, where the corresponding separation is maximized (Figure 2c). Continuously, a reduced separation between the contact surfaces will weaken the dipole moment, and free electrons flow back to the copper electrode until the two contact surfaces come into contact (Figure 2d), making a complete cycle of electricity generation process. Consequently, the kinetic energy from the water wave induced consecutive ball collisions result in a periodical-changing electric field that drives reciprocating flows of electrons between electrodes, producing alternating current in the external circuit. The variation of electric potential is visualized *via* COMSOL in Supporting Movie 1.

We first studied the performance of a single unit of TENG for energy harvesting; and a first step was to trigger the minimum functional unit by a ball collision as driven by gravity. A simple measurement platform was established: a 160 g metal ball was controlled to collide at the center of the top plate with tunable acceleration and displacement. A schematic illustration of the measurement platform is presented in Supporting Figure S1. Dependence of the open circuit voltage and short circuit current on the acceleration and displacement of the ball collision are respectively exhibited in Figure 3a,b. As Figure 3a indicated, the voltage amplitude is an increasing function of both acceleration and displacement of the rolling ball. Likewise, the current amplitude follows the same trend, as displayed in Figure 3b. The open circuit voltage and short circuit current, induced by the ball collision at an acceleration of 10 m/s^2 and a displacement of 9 cm, shot up to 569.9 V and 0.93 mA, as respectively shown in the Figure 3c,d. Resistors were utilized as external loads to further investigate the output power under the same condition. As displayed in Figure 3e, the current amplitude drops with increasing load resistance owing to the ohmic loss, while the voltage follows a reverse trend. As a result, the instantaneous peak power is maximized at a load resistance of 1 MΩ, corresponding to a peak power density of 0.26 mW/cm^2 (Figure 3f). Here, a further step was taken to investigate the effectiveness of the synchronization for current output enhancement. Here, the basic unit of the TENG actually is made of two back-to-back functional units separated by a middle acrylic substrate, as illustrated in Supporting Figure S2. As shown in Supporting Figure S3, under the same collision conditions, the current output of the single side of the device is about half of that of the whole device. Likewise, the output power of the single side was also investigated. As demonstrated in Supporting Figure S4, the instantaneous peak power of a single side of the device is maximized at a load resistance of 10 MΩ, with a peak power density of 0.1 mW/cm^2 (Figure 3f). Consequently, the rational structure design can effectively enhance the current output as well as the energy conversion efficiency.

For wave energy harvesting, four basic units, vertically anchored walls, allow a metal ball to form a TENG, as the photograph shows in Figure 4a. Triggered by the water wave motion, the ball at the center of a basic unit will collide with the walls, namely, the standing basic units. A photograph of the water wave is displayed in Supporting Figure S5a. A two-dimensional schematic illustration of the basic working principle of a TENG is demonstrated in Supporting Figure S5b. To develop a TENG-NW, thousands of TENGs will be electrically connected and woven into a network, as the sketch shows in Figure 4b.

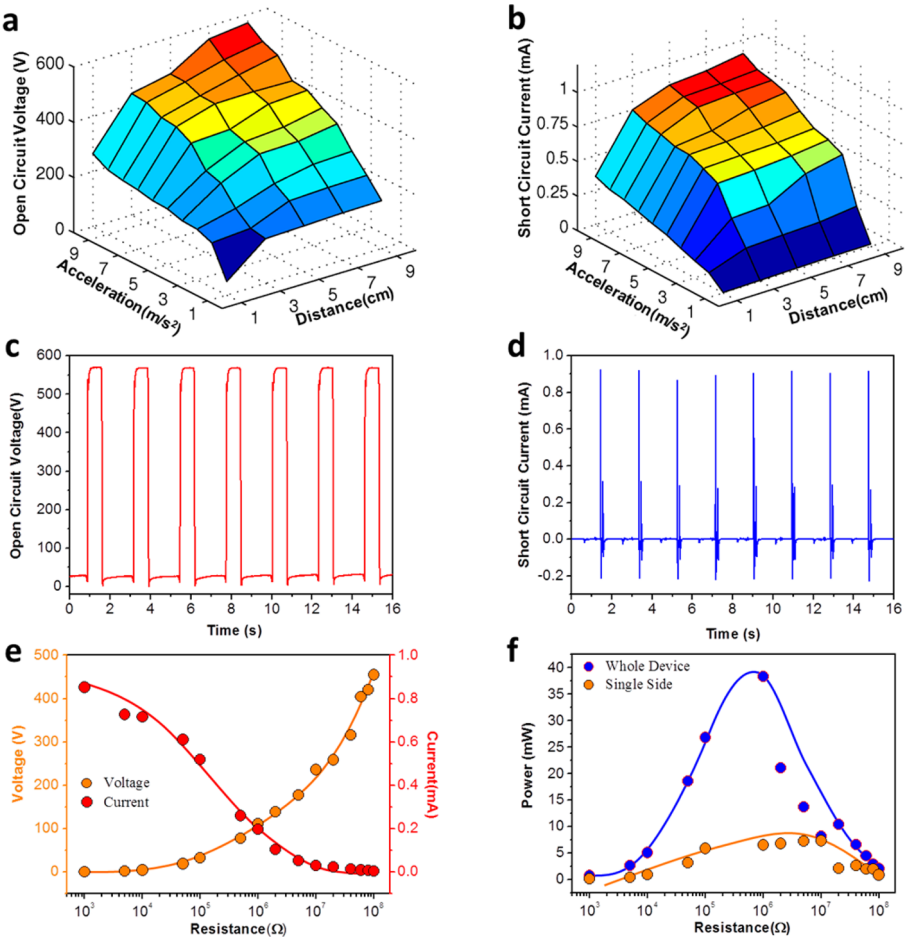

Figure 3. Electrical output characterization of a single unit of TENG. (a) Dependence of the open circuit voltage (a) and short circuit current (b) on the acceleration and displacement of a 160 g metal ball collision. The open circuit voltage (c) and short circuit current (d) induced by the ball collision with an acceleration of 10 m/s^2 and a displacement of 9 cm. (e) Dependence of the voltage and current output on the external load resistance. The points represent peak values of electric signals, while the lines are the fitted results. (f) Dependence of the peak power output on the resistance of the external load. Blue curve is for the whole device, indicating the maximum power output is obtained at 1 MW. The yellow curve is for the single side output, indicating the maximum power output is obtained at 5 MΩ.

To deduce and demonstrate the law of the TENG-NW for blue energy harvesting, a further study was taken to investigate the output performance on the unit numbers. With this regard, four units were fabricated and woven into a small-scale network. As illustrated in Supporting Figure S6, the seesawing motion of the tank with water inside will generate the water wave for experimental measurement. The output characteristics regarding the scale of the TENG-NW were demonstrated in Figure 4c−f. The output current and voltage of the TENG-NW with unit number $n = 1, 2, 3, 4$ were respectively demonstrated in Figure 4c,d. From the evolution of the output signals regarding the increasing of unit numbers, certain trends can be derived for the TENG-NW. First, current amplitudes are drastically increased with elevated unit numbers. The average current amplitude at $n = 1$ is about 50.44 μA, which is greatly increased to 301.95 μA at $n = 4$, as indicated in Figure 4c. Second, the peak density of current output is also obviously increased when the unit number increased from 1 to 4. Enlarged views of the current output signals with different unit numbers are displayed in Supporting Figure S7. Third, the peak density of voltage signals is still an increasing function of the unit number, as displayed in Supporting Figure S8. Here the average voltage peak amplitudes hold almost constant with elevated unit numbers, which is attributed to the electrically parallel-connected units. On the basis of the above observations, it can be inferred that a quasi-direct/direct output signal could be obtained if thousands of units work together as a TENG-NW. Also the output power frequency is totally controllable and tunable by configuration design of the TENG-NW. With a diode bridge, the total accumulative induced charges can also be measured, as show in Figure 4e. A directly proportional relationship was found between the unit number and the charging accumulation rate. This is because more units in the TENG-NW means more collisions are launched in a unit period of time, thus, with faster triboelectric charge generation, higher charging accumulation rate is expected. Additionally, further effort was committed to investigate the dependence of

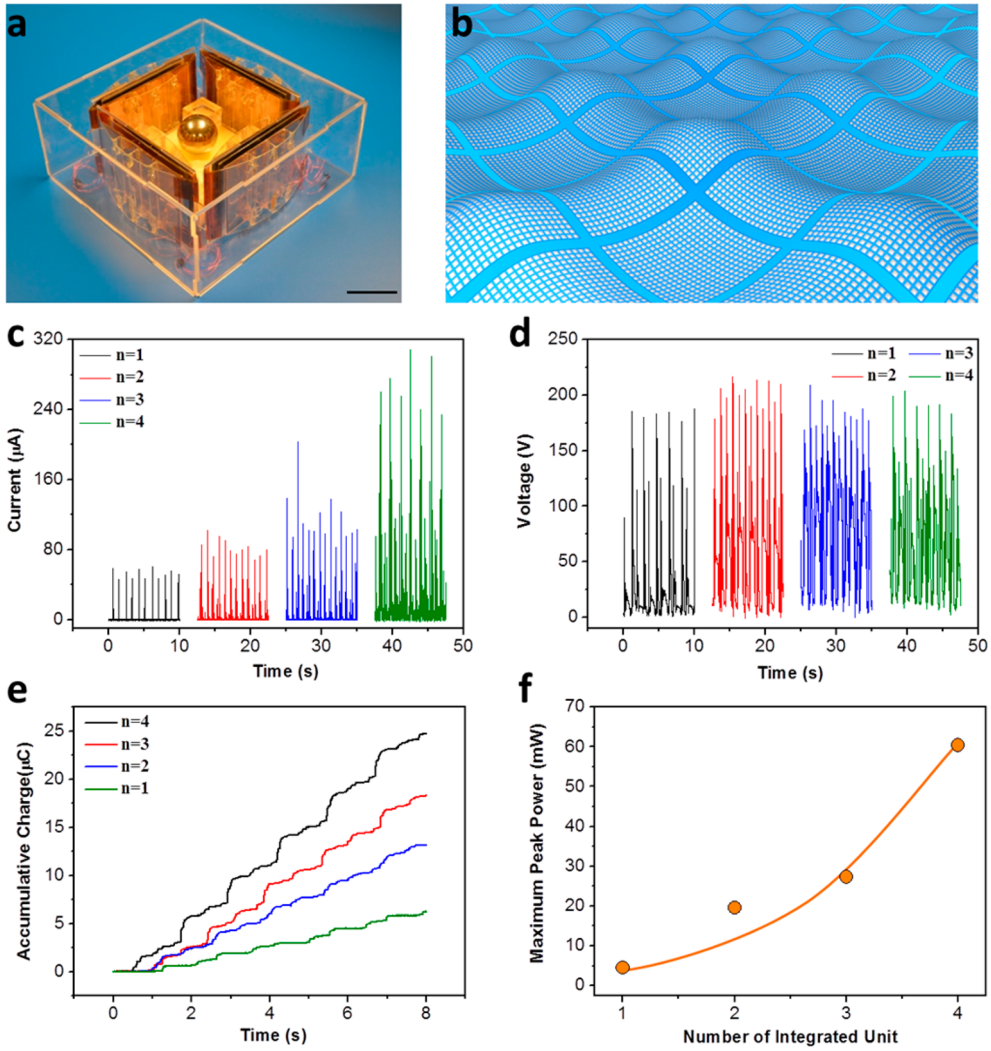

Figure 4. TENG-NW and its electrical output characterization for water wave energy harvesting. (a) Photograph of an as-fabricated single unit of the TENG-NW. The scale bar is 5 cm. (b) Schematic illustration of the TENG-NW that consists of thousands of single units. (c) Rectified short circuit current of the TENG-NWs with unit number n = 1, 2, 3, 4. (d) Open circuit voltage of the TENG-NWs with unit number n = 1, 2, 3, 4. (e) Accumulative induced charges generated by the TENG-NWs with unit number n = 1, 2, 3, 4. (f) Dependence of the peak power output on the resistance of the unit numbers of TENGs. Here, all of the units are electrically connected in parallel.

the peak power output on the resistance of the TENG-NW unit numbers. As demonstrated in Figure 4f, the peak output power of the TENG-NW is exponentially increased with the elevated unit numbers.

To extrapolate the capability of the TENG-NW for large scale blue energy harvesting, the TENG-NW with a single unit was considered. The generated average power E_0 in a single current peak can be calculated as

$$E_0 = \alpha I_{sc} V_{oc} \Delta t \quad (1)$$

where I_{sc} and V_{oc} are the average short-circuit current and open-circuit voltage for the single unit, which are 50 μA and 180 V, respectively; Δt is the peak width of the short-circuit current with a value of 0.0184 s (Supporting Figure S9); and α is a factor in the range of 0 to 1. For a rough estimation, assuming α = 0.5 and submitting all the values into eq 1, E_0 is calculated to be 82.8 μJ.

Regarding a single unit of the TENG-NW, one collision will generate two current peaks with identical $I_{sc}\Delta t$; consequently, the generated average power E_c in one collision can be estimated as

$$E_c = 2E_0 \quad (2)$$

The generated power per second per unit volume E_{cv} can be expressed as

$$E_{cv} = f\beta\frac{E_c}{V_o} \quad (3)$$

where β is the volume ratio of TENG-NW since all of the units in the TENG-NW are not close packed. Here, β is designed to be 0.6. V_o is the effective volume of a single unit. According to the experimental design, V_o = 6 cm × 12 cm × 12 cm = 864 cm^3. f is the ball collision frequency, assuming an average collision frequency is 2 Hz for the ocean wave. Thus, E_{cv} is estimated to be 0.23 J/m^3.

Featured as an extremely lightweight and highly anticorrosive to the marine environment, it is reasonable to construct the TENG-NW with a depth of 5 m in the ocean; then, the generated energy in a water area of 1 km^2 per second could be estimated as

$$E = (5\ m \times 1\ km^2)E_{cv} \quad (4)$$

Submitting eq 3 into eq 4 gives E to be 1.15 MJ.

Consequently, an average power output of 1.15 MW is expected in a water area of 1 km^2 for the reported TENG-NW. To demonstrate its feasibility as a practical power source, a small scale TENG-NW was developed with four units connected in parallel. As displayed in Figure 5a, a small TENG-NW with 4 units is floating on the water surface of a home swimming pool. As a light wind passed by, the aroused gentle wave can start to drive the TENG-NW, which is capable of realizing a self-powered SOS system for ocean emergency, as shown in Figure 5b and Supporting Movie 2. Figure 5c is a schematic illustration of the configuration of the TENG-NW for practical applications. Here, a multilayer electrical connection is proposed. In a foot layer, thousands of single units are electrically connected in parallel to form a community, which could effectively enhance the output current. In the upper layer, thousands of communities could be electrically connected in series to obtain an enhanced output voltage. As a result, the current, voltage, amplitude, and peak density will be greatly boosted up to a high level for practical applications. Compared with current technologies for wave energy harvesting, the TENG-NW holds unprecedented advantages toward large-scale ocean wave energy harvesting. First, TENG-NW is suitable to harvest wave energy in a wide range of wave motions, from subtle to strong, transverse wave to lateral wave. Furthermore, not like the electromagnetic effect based wave energy harvesting, which mainly relies on the undercurrents, the TENGs will show great potential in harvesting energy from both the undercurrent and the surface waves. In addition, most of the wave motions are multidirectional, the TENG-NW, with a rationally designed structure, renders an innovative and effective approach to fully utilize the wave motion from all directions. It can not only be applied in the epicontinental sea but can also easily be implemented in almost all of the water area.

Second, since the TENGs are mostly made from polymer materials without magnets, the load of the total device is expected to be decreased greatly compared to current electromagnetic generators, which are made from heavy materials (such as metals). Moreover, relying on the surface charging effect, only a small amount of materials are needed. The TENG-NW is thus cost-effective as well as lightweight, which makes it possibly highly anticorrosive to the marine environment, and floating on the water surface for wave energy harvesting. This will greatly eliminate the need for building poles or towers for holding traditional electromagnetic generators for wave energy harvesting.

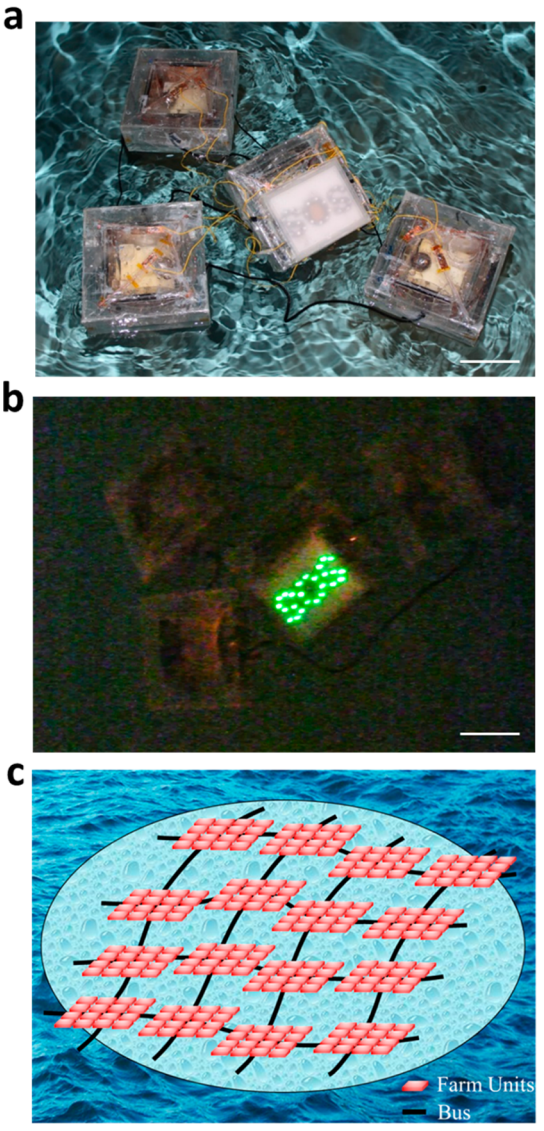

Figure 5. Demonstration of a small scale TENG-NW as a sustainable power source. (a) Photograph of a small scale TENG-NW with 4 units in a swimming pool. The scale bar is 10 cm. (b) Photograph showing that the TENG-NW works and is capable of realizing a self-powered SOS system for ocean emergency. The scale bar is 10 cm. (c) Schematic illustration of the configuration of the proposed TENG-NW for practical applications.

Third, with the network architecture and packaging of individual TENG, the failure rate of the structure could be greatly decreased compared to the state-of-art technologies. Besides, in a case where any of the single units in the TENG-NW was broken, the entire network can tolerate the failed one, and the working status of the rest of the TENGs will not be affected.

In a word, with a distinctive working mechanism and rational designed device structures, the TENG-NW will distinguish itself in the field of energy harvesting with unique applicability, especially playing a

complementary role in the current development of wave energy harvesting.

CONCLUSIONS

Creatively harnessing the surface charging effect between the conventional polymers and very thin layer of metal as electrodes, the triboelectrification-based TENG-NW is featured as lightweight, extremely cost-effective, easily implementated, environmentally friendly, highly anticorrosive to the marine environment, and capable of floating on the water surface. Through rational structural design, the reported TENG-NW excels in conversion of the slow, random, and high-force oscillatory motions into electricity. An average power output of 1.15 MW is expected in a water area of 1 km^2, and a multilayer electrical connection for the TENG-NW is proposed. Resorting to tuning the number of units and communities in the TENG-NW, the current and voltage parameters, including amplitudes, peak density, frequency, and the output power, are designable. From the perspective of system configuration, the TENG-NW concept still paves a unique way in power management for the triboelectrification-based large-scale energy harvesting. Holding a high sensitivity to external wave motion, the presented TENG-NW can not only be used to harvest strong wave motion from ocean but also applied in various other circumstances, where the wave is gentle, such as in a lake, river, or home swimming pool.

In a word, resulting from distinctive mechanism and structure, the TENG-NW presents a possible green and effective route in the fields of water wave energy harvesting. The justified concepts and demonstrations in this work can be immediately and extensively adopted in a variety of applications and can effectively improve the way of our living. In addition, our TENG-NW can serve as the "substrate" and be integrated with wind energy harvesters for various kinds of energies.

METHODS

Fabrication of Nanowires Array on PTFE Surface. (1) A 25 μm thick PTFE film was washed ordinarily with menthol, isopropyl alcohol, and deionized water, then dried with compressed nitrogen; (2) a layer of 100 nm copper was first deposited onto one side of the PTFE film as back electrode; (3) then, a layer of 10 nm thick Au was coated onto the other side of the PTFE film as a nanoscale mask for creating the surface roughness; (4) the Au coated PTFE was placed in an ICP chamber, and O_2, Ar, and CF_4 gases were introduced into the ICP chamber with the flow ratio of 10.0, 15.0, and 30.0 sccm, respectively; (5) a large density of plasma was generated by a power source of 400 W; (6) another power source of 100 W was used to accelerate the plasma ions. The copper coated PFTE film was etched for 60 s to obtain the polymer nanowires.

Nanopore-Based Aluminum Surface Modification. Relying on 3% mass fraction oxalic acid ($H_2C_2O_4$) electrolyte, the electrochemical anodization was applied on the aluminum thin film. It was anodized under bias voltage of 30 V for 5 h with a platinum plate acting as the cathode. After that, the alumina layer was etched away in a solution of chromic acid (20 g/L) at 60 °C for 2 h.

Electrical Measurement. The output voltage signal of the TENG-NW was acquired *via* a voltage preamplifier (Keithley 6514 System Electrometer). The output current signal of the TENG-NW was acquired by a low-noise current preamplifier (Stanford Research SR560).

Conflict of Interest: The authors declare no competing financial interest.

Acknowledgment. Research was supported by the Hightower Chair foundation, and the "Thousands Talents" program for pioneer researcher and his innovation team, China, Beijing City Committee of Science and Technology (Z131100006013004 and Z131100006013005). Patents have been filed based on the research results presented in this manuscript.

Supporting Information Available: (Figure S1) Schematic illustration of the measurement platform to characterize the electrical output of a single unit of TENG; (Figure S2) sketch to show a single side of the device; (Figure S3) current output comparison of the whole device with its single side; (Figure S4) output power of the one side of the minimum functional unit; (Figure S5) working principle of a single unit of the TENG-NW; (Figure S6) sketch showing the water wave generation in the lab for TENG-NW electrical output characterization; (Figure S7) current output characterization of the reported TENG-NW; (Figure S8) voltage output characterization of the reported TENG-NW; (Figures S9) current peak width measurement of the single unit of the TENG-NW; Supporting Movies 1 and 2. This material is available free of charge *via* the Internet at http://pubs.acs.org.

REFERENCES AND NOTES

1. Khaligh, A.; Onar, O. C. *Energy Harvesting: Solar, Wind, and Ocean Energy Conversion Systems*; CRC Press: Boca Raton, FL, 2009.
2. Painuly, J. P. Barriers to Renewable Energy Penetration; A Framework for Analysis. *Renew. Energy* **2001**, *24*, 73–89.
3. Painuly, J. P. *Renewable Energy*; Oxford University Press: Oxford, U.K., 2004.
4. Salter, S. H. Wave Power. *Nature* **1974**, *249*, 720–724.
5. Falcao, A.F. O. Wave Energy Utilization: A Review of the Technologies. *Renew. Sust. Energy Rev.* **2010**, *14*, 899–918.
6. Taylor, G. W.; Burns, J. R.; Kammann, S. M.; Powers, W. B.; Welsh, T. R. The Energy Harvesting Eel: A Small Subsurface Ocean/River Power Generator. *IEEE J. Oceanic Eng.* **2002**, *26*, 539–547.
7. Falnes, J. A Review of Wave-Energy Extraction. *Mar. Struct.* **2007**, *20*, 185–201.
8. Kofoed, J. P.; Frigaard, P.; Friis-Madsen, E.; Sørensen, H. C. Prototype Testing of the Wave Energy Converter Wave Dragon. *Renew. Energy* **2006**, *31*, 181–189.
9. Wang, Z. L. Triboelectric Nanogenerators as New Energy Technology for Self-Powered Systems and as Active Mechanical and Chemical Sensors. *ACS Nano* **2013**, *7*, 9533–9557.
10. Wang, Z. L. Triboelectric Nanogenerators as New Energy Technology and Self-Powered Sensors-Principles, Problems and Perspectives. *Faraday Discuss.* **2015**, 10.1039/C4FD00159A.
11. Wang, Z. L.; Wu, W. Nanotechnology-Enabled Energy Harvesting for Self-Powered Micro-/Nanosystems. *Angew. Chem., Int. Ed.* **2012**, *51*, 11700–11721.
12. Zhu, G.; Peng, B.; Chen, J.; Jing, Q.; Wang, Z. L. Triboelectric Nanogenerators as a New Energy Technology: From Fundamentals, Devices, to Applications. *Nano Energy* **2015**, 10.1016/j.nanoen.2014.11.050.
13. Hou, T. C.; Yang, Y.; Zhang, H.; Chen, J.; Chen, L. J.; Wang, Z. L. Triboelectric Nanogenerator Built Inside Shoe

Insole for Harvesting Walking Energy. *Nano Energy* **2013**, *2*, 856–862.
14. Chen, J.; Zhu, G.; Yang, J.; Jing, Q.; Bai, P.; Yang, W.; Qi, X.; Su, Y.; Wang, Z. L. Personalized Keystroke Dynamics for Self-Powered Human-Machine Interfacing. *ACS Nano* **2015**, *9*, 105–116.
15. Yang, J.; Chen, J.; Liu, Y.; Yang, W.; Su, Y.; Wang, Z. L. Triboelectrification-Based Organic Film Nanogenerator for Acoustic Energy Harvesting and Self-Powered Active Acoustic Sensing. *ACS Nano* **2014**, *8*, 2649–2657.
16. Zhu, G.; Chen, J.; Zhang, T.; Jing, Q.; Wang, Z. L. Radial-Arrayed Rotary Electrification for High Performance Triboelectric Generator. *Nat. Commun.* **2014**, *5*, 3426.
17. Yang, J.; Chen, J.; Yang, Y.; Zhang, H.; Yang, W.; Bai, P.; Su, Y.; Wang, Z. L. Broadband Vibrational Energy Harvesting Based on a Triboelectric Nanogenerator. *Adv. Energy Mater.* **2014**, *4*, 1301322.
18. Zhu, G.; Bai, P.; Chen, J.; Wang, Z. L. Power-Generating Shoe Insole Based on Triboelectric Nanogenerators for Self-Powered Consumer Electronics. *Nano Energy* **2013**, *2*, 688–692.
19. Yang, W.; Chen, J.; Zhu, G.; Wen, X.; Bai, P.; Su, Y.; Lin, Y.; Wang, Z. L. Harvesting Vibration Energy by a Triple-Cantilever Based Triboelectric Nanogenerator. *Nano Res.* **2013**, *6*, 880–886.
20. Zhu, G.; Chen, J.; Liu, Y.; Bai, P.; Zhou, Y.; Jing, Q.; Pan, C.; Wang, Z. L. Linear-Grating Triboelectric Generator Based on Sliding Electrification. *Nano Lett.* **2013**, *13*, 2282–2289.
21. Zhong, J.; Zhong, Q.; Fan, F.; Zhang, Y.; Wang, S.; Hu, B.; Wang, Z. L.; Zhou, J. Finger Typing Driven Triboelectric Nanogenerator and Its Use for Instantaneously Lighting Up LEDs. *Nano Energy* **2013**, *2*, 491–497.
22. Guo, H.; Leng, Q.; He, X.; Wang, M.; Chen, J.; Hu, C.; Xi, Y. A Triboelectric Generator Based on Checker-Like Interdigital Electrodes with a Sandwiched PET Thin Film for Harvesting Sliding Energy in All Directions. *Adv. Energy Mater.* **2015**, *5*, 1400790.
23. Lin, L.; Xie, Y.; Niu, S.; Wang, S.; Yang, P. K.; Wang, Z. L. Robust Triboelectric Nanogenerator Based on Rolling Electrification and Electrostatic Induction at an Instantaneous Energy Conversion Efficiency of∼55%. *ACS Nano* **2015**, *9*, 922–930.
24. Fang, H.; Wu, W.; Song, J.; Wang, Z. L. Controlled Growth of Aligned Polymer Nanowires. *J. Phys. Chem. Lett.* **2009**, *113*, 16571–16574.
25. Yang, W.; Chen, J.; Zhu, G.; Yang, J.; Bai, P.; Su, Y.; Jing, Q.; Cao, X.; Wang, Z. L. Harvesting Energy from Natural Vibration of Human Walking. *ACS Nano* **2013**, *7*, 11317–11324.
26. Chen, J.; Zhu, G.; Yang, W.; Jing, Q.; Bai, P.; Yang, Y.; Hou, T.; Wang, Z. L. Harmonic-Resonator-Based Triboelectric Nanogenerator as a Sustainable Power Source and a Self-Powered Active Vibration Sensor. *Adv. Mater.* **2013**, *25*, 6094–6099.
27. Su, Y.; Zhu, G.; Yang, W.; Yang, J.; Chen, J.; Jing, Q.; Wu, Z.; Jiang, Y.; Wang, Z. L. Triboelectric Sensor for Self-Powered Tracking of Object Motion Inside Tubing. *ACS Nano* **2014**, *8*, 3843–3850.
28. Zhu, G.; Su, Y.; Bai, P.; Chen, J.; Jing, Q.; Yang, W.; Wang, Z. L. Harvesting Water Wave Energy by Asymmetric Screening of Electrostatic Charges on a Nanostructured Hydrophobic Thin-Film Surface. *ACS Nano* **2014**, *8*, 6031–6037.
29. Su, Y.; Wen, X.; Zhu, G.; Yang, J.; Chen, J.; Bai, P.; Wu, Z.; Jiang, Y.; Wang, Z. L. Hybrid Triboelectric Nanogenerator for Harvesting Water Wave Energy and as a Self-Powered Distress Signal Emitter. *Nano Energy* **2014**, *9*, 186–195.
30. Zhang, X. S.; Han, M.; Wang, R.; Zhu, F.; Li, Z.; Wang, W.; Zhang, H. X. Frequency-Multiplication High-Output Triboelectric Nanogenerator for Sustainably Powering Biomedical Microsystems. *Nano Lett.* **2013**, *13*, 1168–1172.
31. Wang, S.; Lin, L.; Wang, Z. L. Nanoscale Triboelectric-Effect-Enabled Energy Conversion for Sustainably Powering Portable Electronics. *Nano Lett.* **2012**, *12*, 6339–6346.
32. Li, Z.; Chen, J.; Yang, J.; Su, Y.; Fan, X.; Wu, Y.; Yu, C.; Wang, Z. L. β-Cyclodextrin Enhanced Triboelectrification for Self-Powered Phenol Detection and Electrochemical Degradation. *Energy Environ. Sci.* **2015**, 10.1039/C4EE03596H.
33. Yang, W.; Chen, J.; Jing, Q.; Yang, J.; Wen, X.; Su, Y.; Zhu, G.; Bai, P.; Wang, Z. L. 3D Stack Integrated Triboelectric Nanogenerator for Harvesting Vibration Energy. *Adv. Funct. Mater.* **2014**, *24*, 4090–4096.
34. Grzybowski, B. A.; Winkleman, A.; Wiles, J. A.; Brumer, Y.; Whitesides, G. M. Electrostatic Self-assembly of Macroscopic Crystals Using Contact Electrification. *Nat. Mater.* **2003**, *2*, 241–245.
35. Yang, W.; Chen, J.; Wen, X.; Jing, Q.; Yang, J.; Su, Y.; Zhu, G.; Wu, W.; Wang, Z. L. Triboelectrification Based Motion Sensor for Human-Machine Interfacing. *ACS Appl. Mater. Interfaces* **2014**, *6*, 7479–7484.
36. Yang, J.; Chen, J.; Su, Y.; Jing, Q.; Li, Z.; Yi, F.; Wen, X.; Wang, Z.; Wang, Z. L. Eardrum-Inspired Active Sensors for Self-Powered Cardiovascular System Characterization and Throat-Attached Anti-interference Voice Recognition. *Adv. Mater.* **2015**, *27*, 1316–1326.